
# Impact of Varying Storm Intensity and Consecutive Dry Days on Grassland Soil Moisture

JOHN D. HOTTENSTEIN

*University of Arizona, Tucson, Arizona*

GUILLERMO E. PONCE-CAMPOS

*Southwest Watershed Research Center, Agricultural Research Service, USDA, and Department of Soil, Water and Environmental Science, University of Arizona, Tucson, Arizona*

JULIO MOGUEL-YANES

*Universidad Juárez Autónoma de Tabasco, Villahermosa, Tabasco, Mexico*

M. SUSAN MORAN

*Southwest Watershed Research Center, Agricultural Research Service, USDA, Tucson, Arizona*

(Manuscript received 20 March 2014, in final form 20 October 2014)

ABSTRACT

Intra-annual precipitation patterns are expected to shift toward more intense storms and longer dry periods because of changes in climate within future decades. Using satellite-derived estimates of plant growth combined with in situ measurements of precipitation and soil moisture between 1999 and 2013, this study quantified the relationship between intra-annual precipitation patterns, annual average soil moisture (at 5-cm depth), and plant growth at nine grassland sites across the southern United States. Results showed a fundamental difference in the response to varying precipitation patterns between mesic and semiarid grasslands. Surface soil moisture in mesic grasslands decreased with an increase of high-intensity storms, whereas in semiarid grasslands, soil moisture decreased with longer dry periods. For these sites, annual average soil moisture was a better indicator of grassland production than total annual precipitation. This improved ability to predict variability in soil moisture and plant growth with changing hydroclimatic conditions will result in more efficient resource management and better-informed policy decisions.

## 1. Introduction

Soil moisture plays an integral role within the hydrologic cycle as a critical link between soils, climate, and biogeography (Legates et al. 2011). Soil moisture has been shown to influence soil respiration (Geng et al. 2012), act as a thermal reservoir that impacts cloud formation and wind fields (Ek and Holtslag 2004; Findell and Eltahir 2003; Entekhabi et al. 1996), and directly influence precipitation formation (Koster et al. 2004). As the understanding of the importance of soil moisture within an ecosystem increases, the effect precipitation patterns have on the ability of rainfall to infiltrate into the soil becomes an important area of study. If the relationship of intra-annual precipitation events on soil moisture can be better understood, models of precipitation and soil moisture can be improved.

Climates across the world are undergoing unprecedented changes. While global precipitation has been reported to exceed the 1961–90 average every year since 1995 (Dore 2005), climatic variability at the local scale is shifting toward intra-annual patterns of extreme weather such as longer growing seasons, larger

*Corresponding author address:* M. Susan Moran, USDA–ARS, Southwest Watershed Research Center, 2000 E. Allen Rd., Tucson, AZ 85719.
E-mail: susan.moran@ars.usda.gov

DOI: 10.1175/JHM-D-14-0057.1

temperature ranges, increased storm intensity, and longer dry periods (Frich et al. 2002; Zhang et al. 2013; Easterling et al. 2000). In the early twenty-first century, grassland regions of the United States have experienced a prolonged warm drought (MacDonald 2010) and a shift to larger, more infrequent storms (Moran et al. 2014). This has raised concern because grasslands have the capacity to respond, through shifts in water use efficiency and biomass production, to variability in precipitation patterns. In fact, there is evidence that grasslands may be the most responsive biome to future climate changes (Ponce-Campos et al. 2013).

Recent studies of the impact of intra-annual rainfall variability on grassland productivity have been based almost exclusively on simulation of increased event size and longer within-season drought periods. Results have shown that a shift toward more intense storms will have a significant impact on grassland soil moisture and, consequently, on aboveground net primary production (ANPP). In semiarid regions, manipulated studies have shown that a shift to fewer but larger events, with no change in total rainfall, led to greater soil water content at depths of 20 cm (Heisler-White et al. 2008). In mesic regions, longer dry intervals between events led to below-average soil water content (Heisler-White et al. 2009; Knapp et al. 2002). These changes in soil moisture were sufficient to increase ANPP in arid grassland by 30% and decrease ANPP in mesic grassland by 18%. Fay et al. (2008) found that the response of grassland ecosystems to extreme rainfall patterns was dependent upon the combination of event size, interval between rainfall events, and total rainfall. It is expected that the sensitivity of grasslands to extreme intra-annual precipitation patterns will be greater during periods of prolonged drought, and particularly in arid regions (Knapp et al. 2002). Cherwin and Knapp (2012) used rainfall manipulations in semiarid grasslands to induce extreme drought and reduce soil moisture at the 20-cm depth; however, they reported that ANPP was not reduced when intra-annual rainfall patterns were characterized by large rain events.

Though these manipulated experiments provide good insights into the mechanisms behind the relation between extreme precipitation patterns and soil moisture, ecosystem responses to precipitation changes are not necessarily a simple combination of the responses of the individual factors (Shaw et al. 2002; Zhang et al. 2013; Knapp et al. 2008). Conditions that affect soil moisture and increase production through 2 years can cause simplifications in the food web after 5 years (Suttle et al. 2007). Chronic intense storms will alter both the mean and temporal variability of soil moisture, resulting in long-term shifts in community composition (Knapp et al. 2002). Even with extended drought, plants show some potential to increase their water use efficiency to buffer the short-term effects of climate change (Ponce-Campos et al. 2013; Knapp and Smith 2001). Long-term field studies provide the opportunity to study how ecosystems are affected by climatic changes.

There remains some controversy about whether the effects of the storm size or frequency will have greater influence on annual and perennial vegetation in grasslands. In a rainfall simulation experiment in an arid region of Iran, Jankju (2008) reported that the effects of storm size were more significant than storm frequency on plant community composition. In contrast, field studies of grasslands in China have shown that precipitation frequency and the timing of dry days in relation to the event intensity had a significant influence on the ability of soils to store water at depths of 20–40 cm (He et al. 2012; Wu et al. 2012). Wu et al. (2012) concluded in their study of worldwide sites that precipitation frequency is an overlooked or underestimated parameter in the relationship between precipitation and soil moisture because of lack of available data. Cherwin and Knapp (2012) reported a strong inverse relation between sensitivity to drought and event size, where larger events resulted in less sensitivity. They explained that when rainfall events were sufficiently large, ANPP was uncoupled from total precipitation amount.

The objective of this research was to study the impact of varying storm intensity and prolonged dry periods on grassland soil moisture during the early twenty-first-century drought at sites across the southern United States. We hypothesized that there exists a fundamental difference in the soil moisture response to extreme precipitation patterns between mesic and semiarid precipitation regimes. This study builds on previously published work, yet it is distinctive in several ways. It is one of only a few studies to include consistent observations over a range of precipitation from semiarid to mesic regimes. It is also one of the first studies to address this objective with long-term observations, in this case extending from 1999 to 2013. Instead of studying the soil moisture at depths 20–30 cm, this study is based on measurements at 5-cm depth for two reasons. First, the bulk of grassland root biomass is reported to be in the top 0–10 cm of the soil, that is, ~50% in mesic grasslands and up to 90% in semiarid systems (Knapp et al. 2002; Cox et al. 1986). Second, the currently orbiting Soil Moisture Ocean Salinity (SMOS) and planned Soil Moisture Active Passive (SMAP) sensors will provide global measurements of soil moisture at this depth (Kerr et al. 2001; Entekhabi et al. 2010).

## 2. Methods

### a. Study sites and data selection

Nine sites were selected across the southern United States (Fig. 1), composed of seven Natural Resources

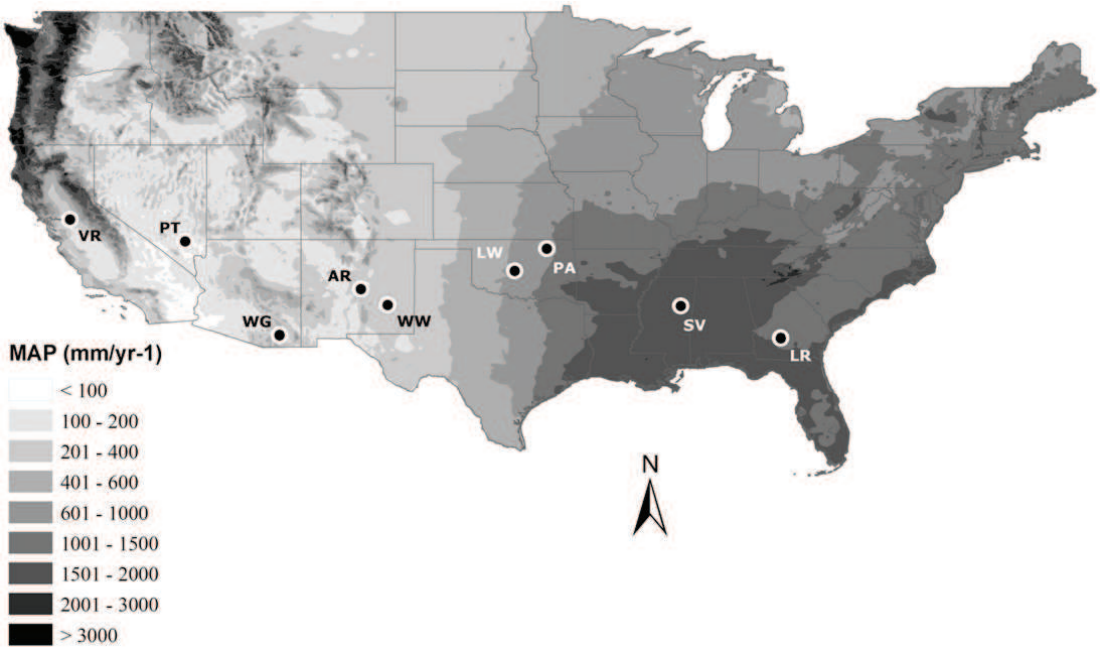


FIG. 1. Distribution of study sites across the southern United States. Sites with lettering in white are mesic and sites with lettering in black are semiarid.

Conservation Service (NRCS) Soil Climate Analysis Network (SCAN) stations, one U.S. Department of Energy (DOE) Atmospheric Radiation Measurement (ARM) site, and one DOE AmeriFlux site (Baldocchi et al. 2004). The data were obtained from the International Soil Moisture Network (ISMN), and within this network, all data were subjected to automated quality control to ensure reliability of the dataset (Dorigo et al. 2013). Locations of sites ranged from a small grassland field approximately 150 m × 200 m to a site surrounded by everal square kilometers of grassland or scrubland (Table 1). All locations were classified as either mesic or semiarid according to their mean annual precipitation $\overline{P}_a$ during the study period between 1999 and 2013. That is, sites with $\overline{P}_a \geq 500$ mm were considered mesic (Starkville, Little River, Little Washita, and Pawhuska) and sites with $\overline{P}_a < 500$ mm were classified as semiarid (Adams Ranch, Pinenut, Vaira Ranch, Willow Wells, and Walnut Gulch). Additionally, the NRCS Web Soil Survey (WSS) was used to determine the field capacity $\Theta_F$ and soil

TABLE 1. Site locations and descriptions. The EVI site column designates sites where MODIS EVI data were obtained and used for analysis.

| Site | | | | | | | |
|---|---|---|---|---|---|---|---|
| Name | Abbreviation | Network | Vegetation classification | Precipitation regime | $\overline{P}_a$ (mm) | EVI site | Soil texture |
| Starkville, MS | SV | SCAN | Agricultural pasture | Mesic | 1521 | — | Loam |
| Little River, GA | LR | SCAN | Agricultural pasture | Mesic | 1069 | — | Loamy sand |
| Little Washita, OK | LW | SCAN | Temperate and boreal shrubland and grassland | Mesic | 826 | X | Loam |
| Pawhuska, OK | PA | ARM | Temperate and boreal shrubland and grassland | Mesic | 804 | X | Loam |
| Adams Ranch, NM | AR | SCAN | Temperate and boreal shrubland and grassland | Semiarid | 319 | X | Loam |
| Pinenut, NV | PT | SCAN | Warm semidesert scrub and grassland | Semiarid | 277 | X | Sandy loam |
| Vaira Ranch, CA | VR | FLUXNET (AmeriFlux) | Mediterranean scrub and grassland | Semiarid | 275 | — | Silt loam |
| Willow Wells, NM | WW | SCAN | Temperate and boreal shrubland and grassland | Semiarid | 259 | X | Sandy loam |
| Walnut Gulch, AZ | WG | SCAN | Warm semidesert scrub and grassland | Semiarid | 258 | — | Sandy loam |

texture at each site (NRCS 2014). The WSS records $\Theta_F$ as an estimate derived from the water content retained at a pressure of ⅓ bar. The soil texture at semiarid sites was predominately sandy loam with two sites classified as silt loam and loam, while the soil texture at mesic sites was predominately loam with one site classified as loamy sand.

The soil moisture and climate datasets were obtained from in situ weather stations that measure daily precipitation and soil moisture at 5-cm depth. At SCAN sites, soil moisture was also measured at 20-cm depth. The soil moisture was measured with different sensors depending on the network being used. SCAN sites utilized an analog or digital HydraProbe sensor, the ARM site utilized a Campbell Scientific Model 229L Matric Potential Sensor, and the AmeriFlux site utilized the Delta-T ThetaProbe ML2. The SCAN HydraProbe has a reported accuracy of $\pm 0.013\,m^3\,m^{-3}$ (Seyfried et al. 2005). The ARM Matric Potential Sensor and AmeriFlux ThetaProbe both claim an accuracy of $\pm 0.05\,m^3\,m^{-3}$ (Schneider et al. 2003; Delta-T Devices 2014).

Daily precipitation data were compiled from rain gauges at the same location as the soil moisture probes. Rain gauges for SCAN sites consisted of tipping buckets or storage-type rain gauges. SCAN precipitation data were given in cumulative amounts and daily rainfall data were obtained by subtracting the annual cumulative total from the previous day's annual cumulative total. Daily precipitation data from the ARM and AmeriFlux networks were collected using a tipping-bucket rain gauge.

Even with a quality-controlled dataset, oftentimes sites had periods of missing or unreported data. The threshold for discarding a year of data because of unreported soil moisture or precipitation was set at 31 continuous days. The 31-continuous-day threshold allowed less than 10% of the yearly missing data to be interpolated to create a complete year of representational data. Soil moisture data were interpolated by averaging the soil moisture values from reported values on dates before and after data were missing. Interpolation to fill gaps in data for soil moisture needed to be done in approximately 155 instances; approximately 143 of those times were for 1- or 2-day periods. For the other 12 times, soil moisture data were interpolated for time periods between 3 and 16 days.

If precipitation data were missing for 1 day and there was a change in the accumulated precipitation value from before and after the unreported data, we recorded that the difference in the accumulated values was the amount of precipitation that fell on the unreported date. For the approximately 11 times precipitation data were missing between 2 and 31 days, precipitation data gaps were filled using a two-step process. First, we made a calculation of the precipitation that fell during the period that data that were missing. This was accomplished by subtracting the annual cumulative precipitation value immediately after reliable data were reported from the annual cumulative precipitation immediately before the station began to report errors. If the precipitation that fell during this time period was $>1$ mm, the total amount of precipitation that fell during the missing gap was then temporally distributed in levels as storms and dry periods based on precipitation records from weather stations within 30 km operated by the National Oceanic and Atmospheric Administration and accessed through the National Climatic Data Center.

### b. *Satellite data*

To study the ecosystem effects of soil moisture on biomass production, the NASA Moderate Resolution Imaging Spectroradiometer (MODIS) enhanced vegetation index (EVI) was used as a cross-site indicator of plant activity (Huete et al. 2002). The dataset for this study was taken from the MODIS product subset MOD13Q1 over the time period from 2001 to 2013. A footprint of 2.25 km $\times$ 2.25 km (9 $\times$ 9 pixels) was obtained over a homogenous area, where the EVI data could then be averaged to produce a single value representative of the in situ measurements (Table 1). If a site was not surrounded by a homogeneous area large enough for the MODIS footprint, EVI data were not retrieved. MODIS data utilize a pixel-based quality assurance scheme to limit noise from aerosols or other atmospheric interference within the dataset. Software developed by Jönsson and Eklundh (2004) was then used to further smooth the dataset before integrating between the start and end of the growing season to produce a proxy for the ANPP known as the integrated EVI iEVI. The iEVI value has been shown to be a reasonable approximation of ANPP (Zhang et al. 2013; Ponce-Campos et al. 2013).

The SMOS satellite provides global soil moisture measurements once every 3 days with an expected accuracy of $0.04\,m^3\,m^{-3}$. One pixel of SMOS data covers approximately 50 km $\times$ 50 km on the ground, an area far greater than what is obtained from the in situ soil moisture probes (Barre et al. 2008). SMOS data were obtained in the form of the level 3 (L3) product from the Centre Aval de Traitement des Données SMOS (CATDS), operated for the Centre National d'Études Spatiales (CNES; France) by the Institut français de recherche pour l'exploitation de la mer (IFREMER; Brest, France). The level-3 soil moisture ($m^3\,m^{-3}$) global data are a 1-day product and contain filtered data gridded at 25-km spatial resolution. The best estimation of soil moisture and dielectric constant are selected (based on the minimization of the data quality index) for each node when several multiorbit retrievals are available for a given soil moisture

User Data Product (UDP). Once data were acquired using the in situ locations, soil moisture values were extracted from the ascending measurements for the 2011, 2012, and 2013 hydrologic years. There were 10 site years where both SMOS and in situ probe measurements were available at each site over the same timeframe that allowed for direct comparison.

### c. Data analysis

Mean annual soil moisture at 5-cm $\overline{\Theta}_a$ and total annual precipitation $P_a$ were used for each hydrologic year available from 1999 to 2013 at each site to derive the two main metrics of our study. To recognize common patterns in the temporal relationship between precipitation and soil moisture, the precipitation and soil moisture values were normalized using the $z$ score. This statistic allows data to be compared for generalized relationships across time for all sites. The long-term annual soil moisture mean at 5 cm $\overline{\Theta}_{a_l}$, mean annual precipitation, and the standard deviation $S_{\overline{\Theta}_a}$ or $S_{P_a}$ from each site between 1999 and 2013 were used to create soil moisture and precipitation $z$ scores, later referred to as normalized soil moisture at 5 cm $\overline{\Theta}_{a_n}$ and normalized precipitation $P_{a_n}$, where

$$\overline{\Theta}_{a_n} = \frac{\overline{\Theta}_a - \overline{\Theta}_{a_l}}{S_{\overline{\Theta}_a}} \tag{1}$$

and

$$P_{a_n} = \frac{P_a - \overline{P}_a}{S_{P_a}}. \tag{2}$$

For each year and site, precipitation data were processed to determine the maximum consecutive dry day length CDD and the simple daily intensity index SDII as defined by Frich et al. (2002). CDD is the maximum length of consecutive dry days over the year, where

$$\text{CDD} = \text{Max No. of consecutive days with precipitation} < 1\,\text{mm day}^{-1}. \tag{3}$$

SDII is an indicator for the value of the average storm intensity (mm day$^{-1}$) throughout the year. SDII is derived from the annual precipitation divided by the number of days with precipitation greater than 1 mm, where

$$\text{SDII} = \frac{P_a}{\text{No. of days with precipitation} \geq 1\,\text{mm}}. \tag{4}$$

SDII is a proxy for actual storm intensity because it is based on daily precipitation over the course of the year. A day with 10 mm of precipitation in a ½ h will have the same SDII value as 10 mm of precipitation over 5 h, even though the two storms would impact soil moisture very differently. Therefore, changes in SDII may be related to shifts from less intense winter rainfall to more intense summer rainfall. To address if changes in precipitation in the cool seasons, versus the warm seasons, were correlated with SDII, we computed the percentage $P_a$ between October and March $P_{C\%}$. This was done by summing the precipitation amounts between October and March $P_C$ and dividing by $P_a$, where

$$P_{C\%} = \frac{P_C}{P_a}. \tag{5}$$

TABLE 2. Summary of high and low SDII and CDD classifications.

| Index | Units | Classification | Mesic | Semiarid |
|---|---|---|---|---|
| CDD | days | Low | ≤25.0 | ≤75.0 |
| | | High | >25.0 | >75.0 |
| SDII | mm day$^{-1}$ | Low | ≤12.5 | ≤7.0 |
| | | High | >12.5 | >7.0 |

CDD and SDII were used to classify each year at each site into high or low CDD and SDII. This followed previous work by Zhang et al. (2013), where the relationship between iEVI and annual precipitation was found to be affected by high and low storm intensity. The demarcations between high and low SDII and CDD were determined according to the median value of SDII and CDD for mesic and semiarid sites, thus retaining a similar number of site years within each classification. The median for SDII in mesic sites was 12.49 mm day$^{-1}$, and from this value, high and low mesic SDII were classified as above and below 12.50 mm day$^{-1}$, respectively. The median for SDII in semiarid sites was 7.22 mm day$^{-1}$, creating a boundary between high and low SDII at 7.00 mm day$^{-1}$. In semiarid sites, the median CDD was 72.5 days, which gave the high and low CDD split at 75 days. Meanwhile, the median of mesic CDD was 24.5 days and the distinction between high and low CDD was 25 days (Table 2).

CDD and SDII were also normalized to minimize the site-to-site bias of longer CDD periods or inherently higher SDII values associated with different precipitation regimes. CDD and SDII were normalized with the mean $\overline{\text{CDD}}$ and $\overline{\text{SDII}}$, and the standard deviation $S_{\text{CDD}}$ and $S_{\text{SDII}}$ from each site, where

$$\text{CDD}_n = \frac{\text{CDD} - \overline{\text{CDD}}}{S_{\text{CDD}}} \tag{6}$$

and

$$\text{SDII}_n = \frac{\text{SDII} - \overline{\text{SDII}}}{S_{\text{SDII}}}. \tag{7}$$

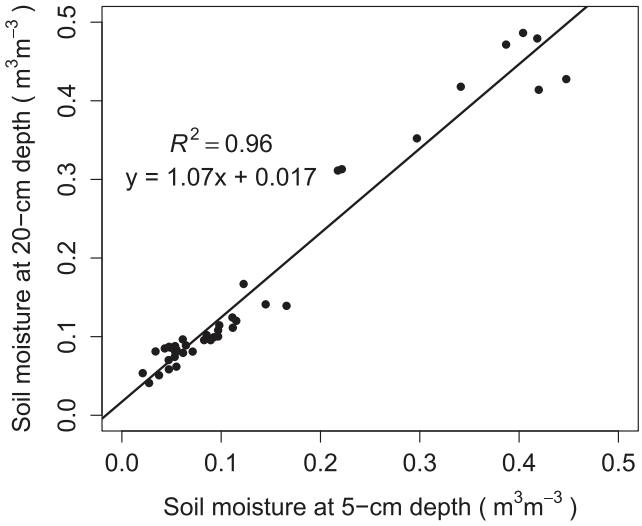


FIG. 2. The linear relationship between mean annual soil moisture observed at 5- and 20-cm depths over the dataset when both observations were available ($n = 40$).

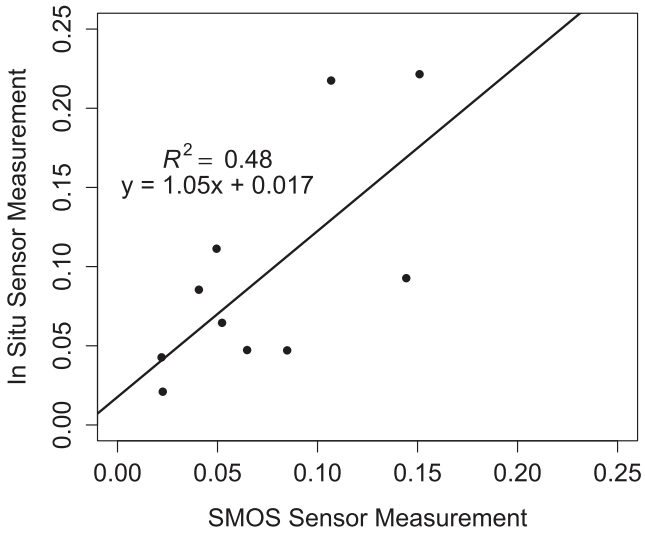


FIG. 3. Linear regression of mean annual soil moisture ($cm^3\,cm^{-3}$) measurements at 5-cm depth obtained from the SMOS satellite and from in situ probes within the SCAN network when both SMOS and in situ measurements were available ($n = 10$, $p < 0.05$).

These variables $\mathrm{CDD}_n$ and $\mathrm{SDII}_n$ were then used to determine their cross-site relation with normalized mean annual soil moisture and an assumed linear relationship, where

$$\overline{\Theta}_{a_n} = a(P_{a_n}) + b(\mathrm{CDD}_n) + c(\mathrm{SDII}_n), \quad (8)$$

$$\overline{\Theta}_{a_n} = d(P_{a_n}) + e(\mathrm{SDII}_n), \quad (9)$$

and

$$\overline{\Theta}_{a_n} = f(P_{a_n}) + g(\mathrm{CDD}_n). \quad (10)$$

First, a generalized linear relationship between soil moisture and precipitation was found both across sites and within sites. Second, to evaluate the interaction of CDD and SDII on the relationship between soil moisture and precipitation at mesic and semiarid locations, sites were analyzed by comparing the linear regressions of ungrouped normalized soil moisture and normalized precipitation data to the linear regressions of grouped data with similar precipitation patterns, that is, high or low CDD and SDII. The linear regressions of the high or low CDD and SDII were tested with analysis of variance (ANOVA) to determine if the CDD and SDII term was significant, based on differences in their slopes or $y$ intercepts. Third, the normalized CDD and SDII values were also used as continuous variables to see if they were significant within a linear regression to explain normalized soil moisture. Finally, the effects of high or low CDD and SDII on normalized mean annual soil moisture were addressed with a two-sided Student's $t$ test.

## 3. Results and discussion

### a. *Extent and depth of annual average soil moisture values*

A basic premise of this study was that the results obtained with soil moisture measurements at 5-cm depth would compare well with previously reported results based on measurements at 20-cm depth. At the SCAN sites where mean annual soil moisture at 5- and 20-cm depths were available over the same annual period ($n = 40$), the soil moisture at the two depths was strongly correlated (coefficient of determination $R^2 = 0.96$, $p < 0.001$; Fig. 2). The high correlation between mean annual soil moisture at 5- and 20-cm depths provided confidence in the ability of the 5-cm soil moisture to be representative of soil moisture at lower depths at these grassland sites at the annual time scale.

In addition, our decision to use soil moisture measured at 5-cm depth was based partly on the fact that the currently orbiting SMOS, launched in 2009, and planned SMAP sensors will provide global measurements of soil moisture at this depth. For the SMOS and in situ measurements where both datasets were of good quality and available over the same timeframe ($n = 10$), we found a reasonable relationship ($R^2 = 0.48$, $p = 0.027$) between $\overline{\Theta}_a$ and the 50 km × 50 km footprint of annual mean soil moisture data obtained from the SMOS satellite (Fig. 3). Considering the difference in scale, this gives some credibility to interpreting the results obtained herein for application with satellite-based measurements by SMOS and SMAP sensors, as well as a general understanding for how well the point-based

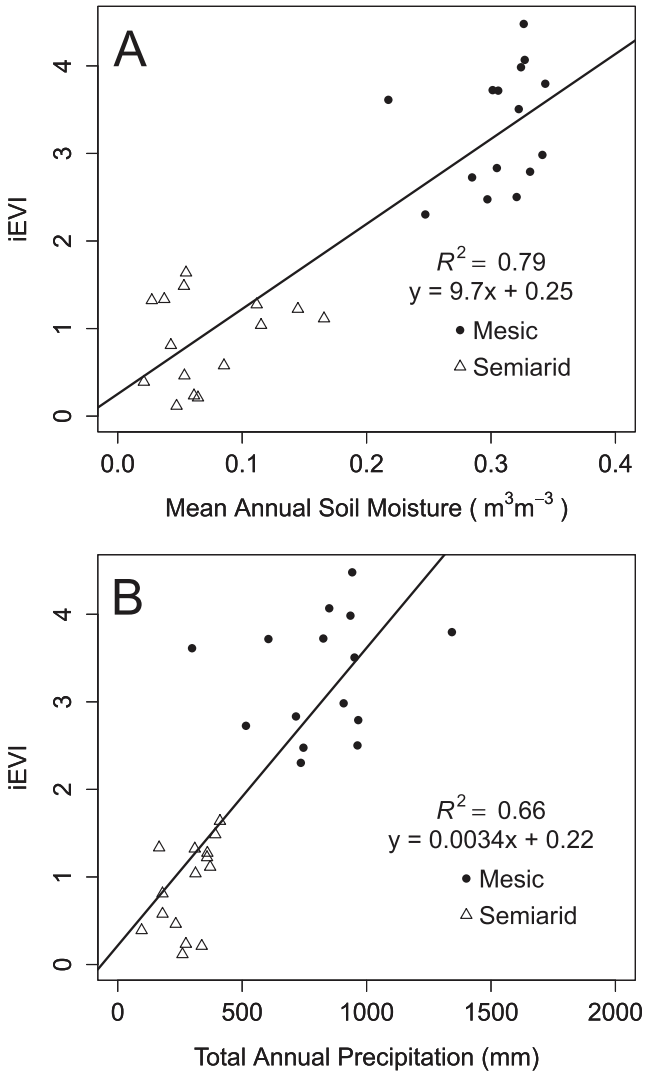


FIG. 4. The relationship between iEVI and (a) soil moisture at 5-cm depth and (b) precipitation. Data are given for sites where iEVI was available ($n$ = 30).

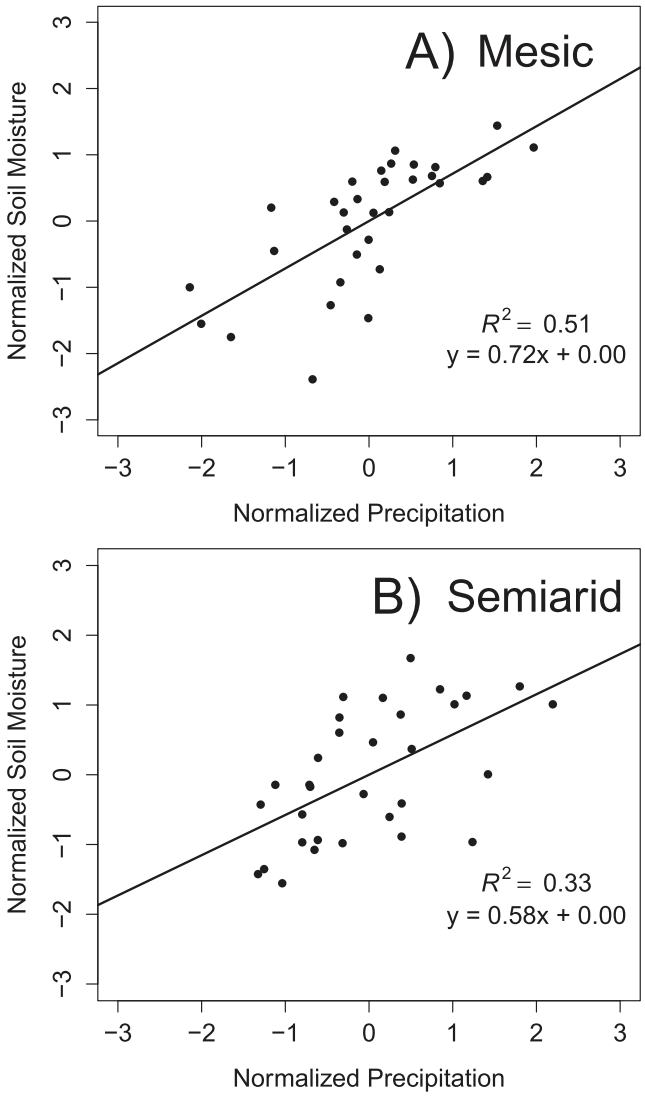


FIG. 5. Linear regression of normalized mean annual soil moisture and normalized annual precipitation for (a) mesic and (b) semiarid sites, where each data point represents a site year ($n$ = 32 for each precipitation regime).

measurements from soil moisture probes are representative of field-scale soil moisture values that ultimately affect plant production.

### b. *Cross-site* $\overline{\Theta}_a$–$P_a$ *and* $\overline{\Theta}_a$–iEVI *spatial relationships*

Across sites where iEVI was available, we found that $\overline{\Theta}_a$ was strongly related to iEVI where sites with lower soil moisture supported lower ANPP, as indicated by low iEVI values (Fig. 4a; $R^2 = 0.79$, $p < 0.001$). The correlation between $P_a$ and iEVI (Fig. 4b; $R^2 = 0.66$, $p < 0.001$) was weaker than between $\overline{\Theta}_a$ and iEVI. Two outlying points of higher iEVI decreased the correlation between iEVI and $P_a$, while soil moisture was able to reconcile the same two points within a single linear regression that has a higher correlation between iEVI and $\overline{\Theta}_a$ than between iEVI and $P_a$. This demonstrated that mean annual soil moisture was likely a better indicator of plant production than total annual precipitation at these sites.

The general within-site temporal relationship between soil moisture and precipitation was studied by using the normalized values of soil moisture and precipitation. For both mesic and semiarid sites, there were weak but significant correlations between $\overline{\Theta}_{a_n}$ and $P_{a_n}$ (Fig. 5; $R^2 = 0.51$ and $R^2 = 0.33$, respectively; $p < 0.001$). The scatter in these relations is partly explained by the additional impact of precipitation patterns (i.e., SDII and CDD) on soil moisture.

### c. SDII *influence on linear* $\overline{\Theta}_{a_n}$–$P_{a_n}$ *relationship*

For mesic sites, $\overline{\Theta}_{a_n}$ and $P_{a_n}$ data classified by high and low SDII were less dispersed along the respective

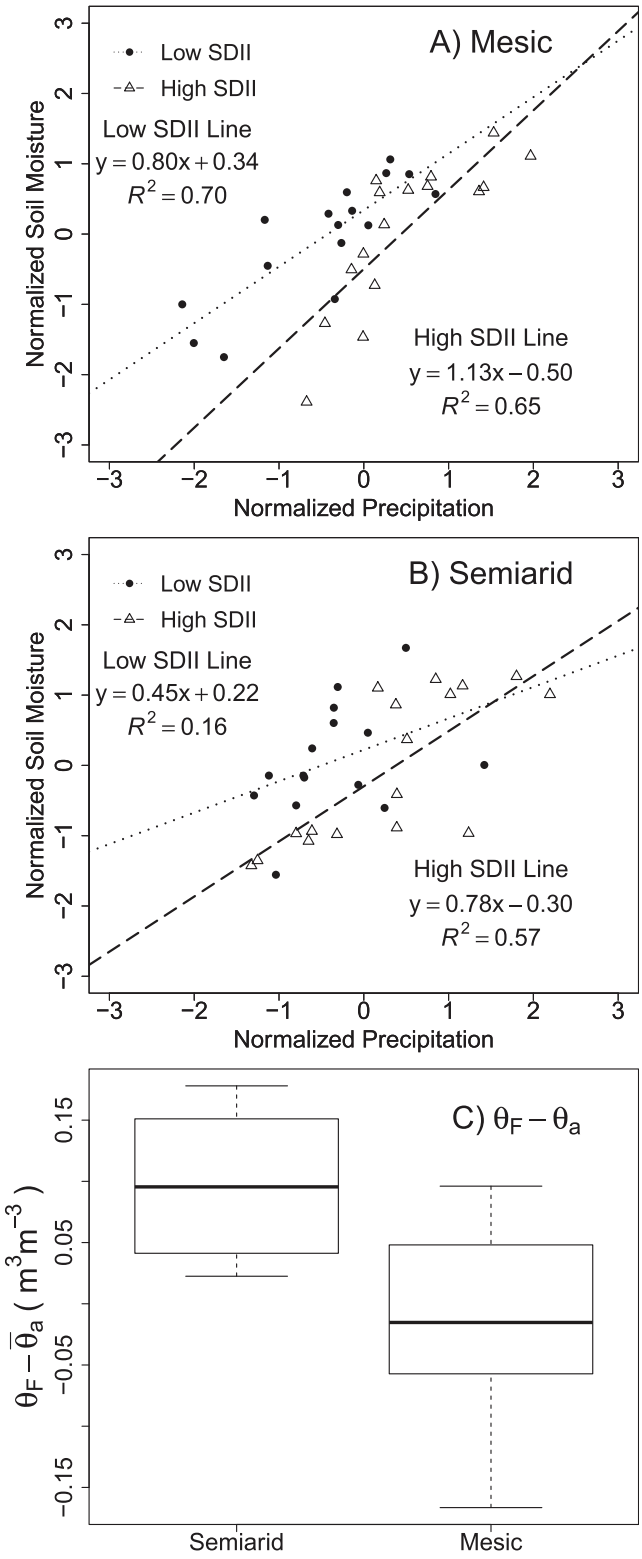


FIG. 6. Linear regression of normalized mean annual soil moisture and normalized annual precipitation for (a) mesic ($n$ = 32) and (b) semiarid sites ($n$ = 32), where sites were classified into high and low SDII as described in Table 2. (c) The distribution of the difference between field capacity and mean annual soil moisture ($\Theta_F - \overline{\Theta}_a$) at mesic ($n$ = 32) and semiarid sites ($n$ = 32). The boldface line represents the median, the upper and lower limits of the box represent the first and third quartiles, and the dashed lines extend to the max and min values.

TABLE 3. Linear regression $R^2$ with data combined or split by SDII and CDD. Boldface values indicate significance at $p < 0.05$.

| Precipitation regime | Combined | SDII | | CDD | |
|---|---|---|---|---|---|
| | | Low | High | Low | High |
| Mesic | **0.51** | **0.70** | **0.65** | **0.49** | **0.48** |
| Semiarid | **0.33** | 0.16 | **0.57** | 0.23 | **0.41** |

regression lines, resulting in higher coefficient of determination for classified data versus unclassified data. The linear regression $R^2$ value increased from 0.51 to 0.65 for high SDII and to 0.70 for low SDII (Fig. 6a, Table 3). The intercepts of the high and low SDII regressions differed significantly ($p < 0.01$), while the slopes of each line were not significantly different ($p = 0.218$). The intercept of the high and low SDII regression lines were −0.50 and 0.34, respectively (Fig. 6a). When SDII was kept as a normalized continuous variable to explain $\overline{\Theta}_{a_n}$, $SDII_n$ was found to be significant ($p < 0.01$) in mesic regimes (Table 4). The similar slopes demonstrate that the underlying contribution of precipitation to soil moisture remains unaffected; however, the different intercepts represent a natural decrease of normalized soil moisture values by 0.84. This represented an average difference in soil moisture of 0.02 $m^3 m^{-3}$ in mesic sites or, on average, 10% of the mean annual soil moisture content at these sites.

For semiarid sites, results were inconsistent. For years with high SDII, the correlation between $P_{a_n}$ and $\overline{\Theta}_{a_n}$ increased from $R^2 = 0.33$ to 0.57, whereas for years with low storm intensity, the correlation decreased from $R^2 = 0.33$ to 0.16 (Fig. 6b, Table 3). There was a significant difference in the intercepts between the high and low SDII classification ($p = 0.050$), but there was no significant difference in slopes between each linear regression ($p = 0.319$). Furthermore, when $SDII_n$ was a continuous variable, it did not contribute significantly to the explanation of $\overline{\Theta}_{a_n}$ in semiarid regimes. The low correlation between normalized precipitation and normalized soil moisture at semiarid sites with low SDII may be due to other factors, such as surface temperature or changing vegetation cover that were not taken into account in this study (Legates et al. 2011).

Storm intensity is an important factor in the correlation between $\overline{\Theta}_{a_n}$ and $P_{a_n}$ at mesic sites, but not so at semiarid sites. The unique impact of storm intensity on soil moisture at mesic sites may likely be a result of the difference between $\overline{\Theta}_a$ and $\Theta_F$ at mesic sites. On average, for all mesic sites, $\overline{\Theta}_a$ was 0.013 $m^3 m^{-3}$ above $\Theta_F$. At semiarid sites, the difference between $\overline{\Theta}_a$ and $\Theta_F$ was, on average, 0.10 $m^3 m^{-3}$ below $\Theta_F$ (Fig. 6c). There was a significant difference ($p < 0.001$) between $\overline{\Theta}_a$ and

TABLE 4. Linear regression variable coefficient (VC) estimates for Eqs. (8)–(10) that were identified in section 2c. The $R^2$ is reported in the bottom row for the equation of each column. The $p$ values for each variable are presented in parentheses after the estimated coefficient, and boldface values indicate significance at $p < 0.05$.

| | Eq. (8) | | | Eq. (9) | | | Eq. (10) | | |
|---|---|---|---|---|---|---|---|---|---|
| Variable | VC | Mesic | Semiarid | VC | Mesic | Semiarid | VC | Mesic | Semiarid |
| $P_{a_n}$ | $a$ | **1.01** ($p < 0.01$) | **0.52** ($p = 0.03$) | $d$ | **1.07** ($p < 0.01$) | **0.74** ($p < 0.01$) | $f$ | **0.61** ($p < 0.01$) | **0.47** ($p < 0.01$) |
| $\mathrm{CDD}_n$ | $b$ | −0.09 ($p = 0.51$) | −0.31 ($p = 0.09$) | — | — | — | $g$ | −0.18 ($p = 0.24$) | **−0.33** ($p = 0.03$) |
| $\mathrm{SDII}_n$ | $c$ | **−0.49** ($p < 0.01$) | −0.07 ($p = 0.76$) | $e$ | **−0.51** ($p < 0.01$) | −0.26 ($p = 0.19$) | — | — | — |
| $R^2$ | | 0.64 | 0.44 | | 0.64 | 0.37 | | 0.52 | 0.43 |

$\Theta_F$ at mesic and semiarid sites. This difference caused the precipitation at semiarid sites to be incorporated into the soil and to increase soil moisture regardless of how quickly the precipitation fell. Because of the inherent property of soil moisture at the field capacity at mesic sites, these sites needed more storms with less rainfall per storm, that is, low SDII, to ensure runoff was minimized and more precipitation was absorbed by the soil, resulting in a higher normalized soil moisture value than if that year were to have a high SDII value.

As mentioned previously, SDII is a simplification of storm intensity based on precipitation data available at the daily time scale. The suitability of SDII as a proxy for storm intensity is arguable because of a potential greater influence from shifts between summer and winter precipitation events than actual increases in annual average storm intensity. We found that the correlation between $\mathrm{SDII}_n$ and $P_{C\%}$ was low at semiarid sites ($R = -0.079$) and at mesic sites ($R = -0.109$). Thus, SDII provided a reasonable proxy for storm intensity independent of changes in seasonal precipitation at these sites.

### d. CDD *influence on linear* $\overline{\Theta}_{a_n}$–$P_{a_n}$ *relationship*

For mesic sites, the relation between $\overline{\Theta}_{a_n}$ and $P_{a_n}$ decreased from $R^2 = 0.51$ to 0.48 with high CDD values and to 0.49 with low CDD values (Fig. 7a, Table 3). The slopes and intercepts of each line were not statistically different ($p = 0.998$ and $p = 0.313$, respectively). The analogous regression lines for high and low values of CDD signify that annual soil moisture is insensitive to CDD at mesic sites.

For semiarid sites, classification of years with high or low CDD improved correlation between $P_{a_n}$ and $\overline{\Theta}_{a_n}$ with high CDD and decreased correlation with low CDD (Fig. 7b, Table 3). Compared to the general $\overline{\Theta}_{a_n}$–$P_{a_n}$ relationship, the $R^2$ value increased from 0.33 to 0.41 ($p = 0.010$) with high CDD and yet decreased to 0.22 ($p = 0.054$) with low CDD. The slopes of the regressions of high and low CDD were not different ($p = 0.341$) as soil moisture increased at the same rate per unit of precipitation. The $y$ intercepts of each regression were significantly different ($p = 0.065$). This $p$ value is slightly above the significance level of 0.05; however, it does lead to the assertion that higher CDD lowers soil moisture in semiarid sites and that CDD is an explanatory variable to model $\overline{\Theta}_{a_n}$. This assertion

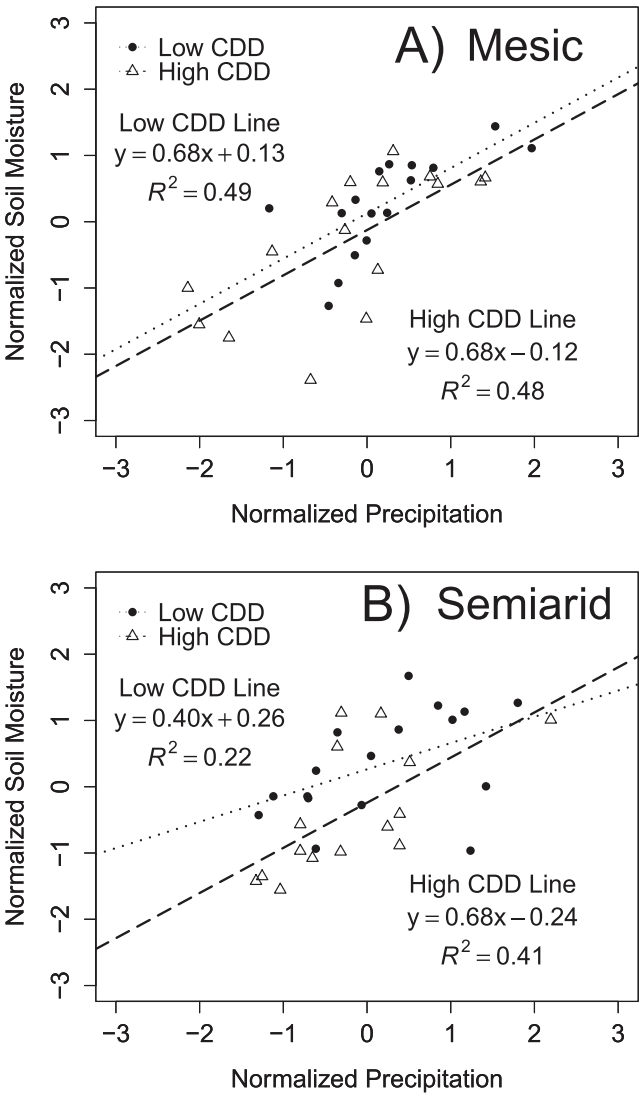


FIG. 7. Linear regression of normalized mean annual soil moisture and normalized annual precipitation for (a) mesic and (b) semiarid sites, where sites were classified into high and low CDD, as described in Table 2 ($n = 32$ for each precipitation regime).

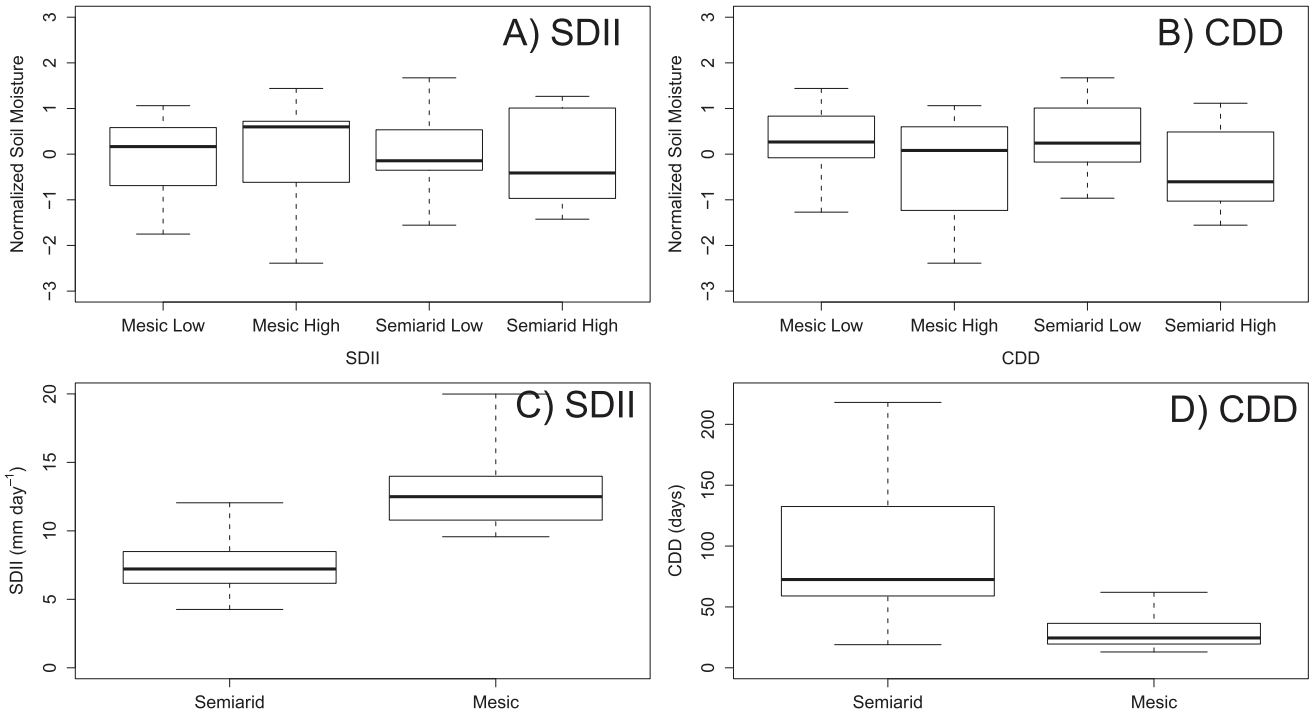


FIG. 8. Boxplots of the normalized mean annual soil moisture for mesic and semiarid sites split by length of (a) SDII and (b) CDD, as described in Table 2. Boxplots broken up by precipitation regime are shown for (c) SDII and (d) CDD. The boldface line represents the median, the upper and lower limits of the box represent the first and third quartiles, and the dashed lines extend to the max and min values ($n = 32$ for each precipitation regime within each boxplot).

was supported when only $CDD_n$ was found to be a significant variable ($p = 0.031$), resulting in an $R^2$ value of 0.43 (Table 4).

### *e.* SDII *and* CDD *effect on* $\overline{\Theta}_{a_n}$

For mesic sites, average $\overline{\Theta}_{a_n}$ was 0.049 with high storm intensity and −0.049 with low storm intensity (Fig. 8a, Table 5). Similar results occurred at the semiarid sites; data classified with high and low storm intensity had average $\overline{\Theta}_{a_n}$ of −0.060 and 0.068, respectively. Averages of mean annual normalized soil moisture with high and low storm intensity at both mesic and semiarid sites were not significantly different ($p = 0.776$ and 0.698, respectively). Similarly, at mesic sites the average $\overline{\Theta}_{a_n}$ with high CDD (−0.28) and low CDD (0.28) were not significantly different ($p = 0.103$). However, for semiarid sites, the average $\overline{\Theta}_{a_n}$ of years with high CDD (−0.38) and low CDD (0.33) differed significantly ($p = 0.033$; Fig. 8b, Table 5) by 0.71 standard deviations. The deviation between high and low CDD represented an average $0.01\,m^3\,m^{-3}$ difference of mean annual soil moisture or 15% of the mean annual moisture content within the soil at semiarid sites.

The unique influence of CDD on semiarid sites and the inability of SDII to influence soil moisture without the incorporation of precipitation may be affected by the difference in the length and variation of CDD or SDII that each regime naturally experiences. Even though SDII values between mesic and semiarid sites were significantly different ($P < 0.001$; Fig. 8c), the SDII influence on soil moisture at mesic sites is codependent with precipitation. On the other hand, semiarid soil moisture was influenced significantly between high and low CDD. This may be a result of semiarid sites experiencing an average CDD of 75 days with a standard deviation of 55.5 days. These values are greater than the mesic sites' average CDD of 28 days, with a standard deviation of 12.1 days. Even the mesic site maximum CDD value of 62 days would place that year with a semiarid low CDD classification (Fig. 8d). With this difference of CDD values that mesic and semiarid sites experience, mesic sites may not be influenced by CDD

TABLE 5. Mean normalized annual soil moisture values broken down by extreme index classification. Boldface values indicate there was a significant difference ($p < 0.05$) between the mean normalized annual soil moisture of high and low CDD or SDII.

| Precipitation regime | Low CDD | High CDD | Low SDII | High SDII |
|---|---|---|---|---|
| Semiarid | **0.33** | **−0.38** | 0.068 | −0.060 |
| Mesic | 0.28 | −0.28 | −0.049 | 0.049 |

because they experience a relatively low CDD and a relatively small variation of CDD.

## 4. Conclusions

For nine grassland sites across the southern United States, we investigated the differing impact of intra-annual patterns of precipitation on soil moisture in mesic and semiarid precipitation regimes. Soil moisture was strongly related to ANPP, as measured by the iEVI. In fact, we found that soil moisture was a better predictor of iEVI than was total precipitation. We also found that our in situ point measurements of soil moisture were correlated to large-scale remotely sensed soil moisture measurements that will allow for increases in the scale of similar studies.

In this study, we addressed the within-site temporal relation between precipitation and soil moisture by normalizing soil moisture and precipitation to units of standard deviation and analyzing the results for the sets of semiarid and mesic sites. We concluded that the precipitation–soil moisture relation was impacted by variations in storm intensity for mesic sites and by the length of consecutive dry days for semiarid sites. This was explained in relation to general climate patterns and the associated distinctions in soil texture in these two precipitation regimes. First, the soil moisture at mesic sites tends to reside closer to field capacity than soil moisture at semiarid sites. So, precipitation associated with high or low storm intensity events will infiltrate into the drier soils at semiarid sites, whereas for mesic sites, precipitation associated with high-intensity storms will result in greater water loss to runoff and less infiltration into soil, compared to low-intensity storms. Second, this field study attributed the length of CDD as having a significant impact on soil moisture only at semiarid sites. This is related to the fact that the variation in length of CDD was naturally low at mesic sites and not variable from year to year, in contrast to the high variability of CDD at semiarid sites. For semiarid sites, long periods of CDD decreased the mean annual soil moisture regardless of the total precipitation throughout the year.

While many factors influence how soil moisture varies with precipitation, this research offers a consistent hydrometeorological explanation for how mesic and semiarid grasslands will be affected by changing precipitation patterns and a changing climate. Incorporation of intra-annual patterns of storm intensity in mesic grasslands and consecutive dry days in semiarid grasslands will help improve estimates of annual soil moisture and better predict grassland production.

*Acknowledgments.* The research was funded and supported by the University of Arizona/Arizona NASA Space Grant Consortium, the NASA SMAP Science Definition Team under Agreement 08-SMAPSDT08-0042, and the University of Arizona Graduate College Latin America Summer Research Program. The SMAP Early Adopter Program provided valuable technical support. We acknowledge the U.S. Department of Energy ARM Climate Research Facility and the USDA SCAN network for making these data available. We would also like to thank Dr. Joe Watkins, University of Arizona Department of Mathematics, for his help in the statistical analysis of our results.

## REFERENCES

Baldocchi, D. D., L. Xu, and N. Kiang, 2004: How plant functional-type, weather, seasonal drought, and soil physical properties alter water and energy fluxes of an oak–grass savanna and an annual grassland. *Agric. For. Meteor.,* **123,** 13–39, doi:10.1016/j.agrformet.2003.11.006.

Barre, H. M. J., B. Duesmann, and Y. H. Kerr, 2008: SMOS: The mission and the system. *IEEE Trans. Geosci. Remote Sens.,* **46,** 587–593, doi:10.1109/TGRS.2008.916264.

Cherwin, K., and A. Knapp, 2012: Unexpected patterns of sensitivity to drought in three semi-arid grasslands. *Oecologia,* **169,** 845–852, doi:10.1007/s00442-011-2235-2.

Cox, J. R., G. W. Frasier, and K. G. Renard, 1986: Biomass distribution at grassland and shrubland sites. *Rangelands,* **8,** 67–68.

Delta-T Devices, cited 2014: ML3 ThetaProbe research data sheet. [Available online at www.delta-t.co.uk/product-support-material.asp.]

Dore, M. H. I., 2005: Climate change and changes in global precipitation patterns: What do we know? *Environ. Int.,* **31,** 1167–1181, doi:10.1016/j.envint.2005.03.004.

Dorigo, W. A., and Coauthors, 2013: Global automated quality control of in situ soil moisture data from the International Soil Moisture Network. *Vadose Zone J.,* **12,** doi:10.2136/vzj2012.0097.

Easterling, D. R., G. A. Meehl, C. Parmesan, S. A. Changnon, T. R. Karl, and L. O. Mearns, 2000: Climate extremes: Observations, modeling, and impacts. *Science,* **289,** 2068–2074, doi:10.1126/science.289.5487.2068.

Ek, M. B., and A. A. M. Holtslag, 2004: Influence of soil moisture on boundary layer cloud development. *J. Hydrometeor.,* **5,** 86–99, doi:10.1175/1525-7541(2004)005<0086:IOSMOB>2.0.CO;2.

Entekhabi, D., I. Rodriguez-Iturbe, and F. Castelli, 1996: Mutual interaction of soil moisture state and atmospheric processes. *J. Hydrol.,* **184,** 3–17, doi:10.1016/0022-1694(95)02965-6.

——, and Coauthors, 2010: The Soil Moisture Active Passive (SMAP) Mission. *Proc. IEEE,* **98,** 704–716, doi:10.1109/JPROC.2010.2043918.

Fay, P. A., D. M. Kaufman, J. B. Nippert, J. D. Carlisle, and C. W. Harper, 2008: Changes in grassland ecosystem function due to extreme rainfall events: Implications for responses to climate change. *Global Change Biol.,* **14,** 1600–1608, doi:10.1111/j.1365-2486.2008.01605.x.

Findell, K. L., and E. A. B. Eltahir, 2003: Atmospheric controls on soil moisture-boundary layer interactions: Three-dimensional wind effects. *J. Geophys. Res.,* **108,** 8385, doi:10.1029/2001JD001515.

Frich, P., L. V. Alexander, P. DellaMarta, B. Gleason, M. Haylock, A. M. G. K. Tank, and T. Peterson, 2002: Observed coherent changes in climatic extremes during the second half of the twentieth century. *Climate Res.,* **19,** 193–212, doi:10.3354/cr019193.

Geng, Y., and Coauthors, 2012: Soil respiration in Tibetan Alpine grasslands: Belowground biomass and soil moisture, but not soil temperature, best explain the large-scale patterns. *PLoS One,* **7,** e34968, doi:10.1371/journal.pone.0034968.

He, Z., W. Zhao, H. Liu, and X. Chang, 2012: The response of soil moisture to rainfall event size in subalpine grassland and meadows in a semi-arid mountain range: A case study in northwestern China's Qilian Mountains. *J. Hydrol.,* **420–421,** 183–190, doi:10.1016/j.jhydrol.2011.11.056.

Heisler-White, J. L., A. K. Knapp, and E. F. Kelly, 2008: Increasing precipitation event size increases aboveground net primary productivity in a semi-arid grassland. *Oecologia,* **158,** 129–140, doi:10.1007/s00442-008-1116-9.

——, J. M. Blair, E. F. Kelly, K. Harmoney, and A. K. Knapp, 2009: Contingent productivity responses to more extreme rainfall regimes across a grassland biome. *Global Change Biol.,* **15,** 2894–2904, doi:10.1111/j.1365-2486.2009.01961.x.

Huete, A., K. Didan, T. Miura, E. P. Rodriguez, X. Gao, and L. G. Ferreira, 2002: Overview of the radiometric and biophysical performance of the MODIS vegetation indices. *Remote Sens. Environ.,* **83,** 195–213, doi:10.1016/S0034-4257(02)00096-2.

Jankju, M., 2008: Individual performances and the interaction between arid land plants affected by the growth season water pulses. *Arid Land Res. Manage.,* **22,** 123–133, doi:10.1080/15324980801957986.

Jönsson, P., and L. Eklundh, 2004: TIMESAT—A program for analyzing time-series of satellite sensor data. *Comput. Geosci.,* **30,** 833–845, doi:10.1016/j.cageo.2004.05.006.

Kerr, Y. H., P. Waldteufel, J.-P. Wigneron, J. Martinuzzi, J. Font, and M. Berger, 2001: Soil moisture retrieval from space: The Soil Moisture and Ocean Salinity (SMOS) mission. *IEEE Trans. Geosci. Remote Sens.,* **39,** 1729–1735, doi:10.1109/36.942551.

Knapp, A. K., and M. D. Smith, 2001: Variation among biomes in temporal dynamics of aboveground primary production. *Science,* **291,** 481–484, doi:10.1126/science.291.5503.481.

——, and Coauthors, 2002: Rainfall variability, carbon cycling, and plant species diversity in a mesic grassland. *Science,* **298,** 2202–2205, doi:10.1126/science.1076347.

——, and Coauthors, 2008: Consequences of more extreme precipitation regimes for terrestrial ecosystems. *Bioscience,* **58,** 811–821, doi:10.1641/B580908.

Koster, R. D., and Coauthors, 2004: Regions of strong coupling between soil moisture and precipitation. *Science,* **305,** 1138–1140, doi:10.1126/science.1100217.

Legates, D. R., R. Mahmood, D. F. Levia, T. L. DeLiberty, S. M. Quiring, C. Houser, and F. E. Nelson, 2011: Soil moisture: A central and unifying theme in physical geography. *Prog. Phys. Geogr.,* **35,** 65–86, doi:10.1177/0309133310386514.

MacDonald, G. M., 2010: Water, climate change, and sustainability in the southwest. *Proc. Natl. Acad. Sci. USA,* **107,** 21 256–21 262, doi:10.1073/pnas.0909651107.

Moran, M. S., and Coauthors, 2014: Change in the function of U.S. grasslands in response to the early 21st century drought. *Ecology,* **95,** 2121–2133, doi:10.1890/13-1687.1.

NRCS, cited 2014: Web Soil Survey. [Available online at http://websoilsurvey.sc.egov.usda.gov/App/HomePage.htm.]

Ponce-Campos, G. E., and Coauthors, 2013: Ecosystem resilience despite large-scale altered hydroclimatic conditions. *Nature,* **494,** 349–352, doi:10.1038/nature11836.

Schneider, J. M., D. K. Fisher, R. L. Elliott, G. O. Brown, and C. P. Bahrmann, 2003: Spatiotemporal variations in soil water: First results from the ARM SGP CART network. *J. Hydrometeor.,* **4,** 106–120, doi:10.1175/1525-7541(2003)004<0106:SVISWF>2.0.CO;2.

Seyfried, M. S., L. E. Grant, E. Du, and K. Humes, 2005: Dielectric loss and calibration of the hydra probe soil water sensor. *Vadose Zone J.,* **4,** 1070, doi:10.2136/vzj2004.0148.

Shaw, M. R., E. S. Zavaleta, N. R. Chiariello, E. E. Cleland, H. A. Mooney, and C. B. Field, 2002: Grassland responses to global environmental changes suppressed by elevated $CO_2$. *Science,* **298,** 1987–1990, doi:10.1126/science.1075312.

Suttle, K. B., M. A. Thomsen, and M. E. Power, 2007: Species interactions reverse grassland responses to changing climate. *Science,* **315,** 640–642, doi:10.1126/science.1136401.

Wu, C., and Coauthors, 2012: An underestimated role of precipitation frequency in regulating summer soil moisture. *Environ. Res. Lett.,* **7,** 024011, doi:10.1088/1748-9326/7/2/024011.

Zhang, Y., and Coauthors, 2013: Extreme precipitation patterns and reductions of terrestrial ecosystem production across biomes. *J. Geophys. Res. Biogeosci.,* **118,** 148–157, doi:10.1029/2012JG002136.